JOURNAL OF OPTOELECTRONICS AND ADVANCED MATERIALS Vol. 9, No. 5, May 2007, p. 1260 - 1264

Growth and optical properties of different compositions of $LiNbO_3$ single crystal fibers

CHI-YUNG CHEN[a*], JYH-CHEN CHEN[a], CHIH-TA CHIA[b]
[a] *Department of Mechanical Engineering, National Central University, Jhong-Li 32001, Taiwan*
[b] *Department of Physics, National Taiwan Normal University, Taipei 116, Taiwan*

In this study the laser-heated pedestal growth (LHPG) method was used to grow lithium niobate ($LiNbO_3$) single crystal fibers with different compositions ratios $[Li_2CO_3]/[Nb_2O_5]$ = 44:56, 45:55, 46:54, 47:53, 48:52, 48.6:51.4, 49:51 and 50:50 achieved by different seed rods. X-ray Single-Crystal Diffractometer (X-Ray/CCD) was used to determine the lattice parameters and crystalline structure of the crystals. The UV absorption spectrum, Fourier-transform infrared spectrometer and Raman scattering spectroscopy results were used to find the optical properties and standard characterization of the different $LiNbO_3$ single crystals. We note that the wavelength of the UV absorption edge and the wave number of the O-H absorption peak were less when the Li_2O composition was large. The plotted results tended to fit a Gaussian curve. The Full-Width Half-Maximum (FWHM) of the Raman peak found at 152 cm^{-1} of the E(TO) mode decreased linearly as the amount of the Li_2O composition increased. The Raman scattering results showed that the structure at the $LiNbO_3$ crystal became more rigid when the amount of the Li_2O composition increased.

(Received November 14, 2006; accepted April 12, 2007)

Keywords: Laser heated pedestal growth method, Lithium niobate, Infrared and Raman spectroscopy, UV absorption spectroscopy

1. Introduction

Lithium niobate ($LiNbO_3$; LN) is a very promising material for optical applications, such as in optical switches, nonlinear optical devices, frequency conversion devices and surface acoustic wave devices. The LN composition was varied by varying the Li_2O composition from 44 to 51 mol% [1, 2]. Congruent LN (CLN) is around 48.6 mol% Li_2O, while stoichiometric LN (SLN) is around 50 mol% Li_2O. They used commercially available LN crystals with a congruent composition, typically grown from a melt using the Czochralski technique. The composition of crystals grown from incongruent LN melts using the typical Czochralski method shows a shift along the growth axis during the growth process [3]. Accurately controlling the incongruent composition of LN crystals using this method is difficult. The flux growth technique has been used to grow bulk incongruent LN crystals from 48.6 to 49.99mol% for a congruent melt doped with different amounts of K_2O[4]. Vapor transport equilibration (VTE) has also been used to change the composition at small incongruent LN crystals from 47 to 50 mol% [5, 6, 7]. It is however difficult to control the composition and the uniformity of the Li_2O composition inside the crystals. Kitamura et al. [8] developed a continuous-charge double-crucible Czochralski (DCCZ) method to grow bulk SLN crystal from a 58 mol% Li-rich melt. Chen et al. [9] used a laser heated pedestal growth (LHPG) technique to grow SLN single crystal fibers from seed rods with different compositions (the LN had Li_2O compositions that varied from 48.6 to 58 mol%), while the feed rods were stoichiometric in composition. The distribution of Li in the grown crystal fiber was detected via Electron Spectroscopy for Chemical Analysis (ESCA). The final equilibrium composition of the crystal fibers was measured by the inductively coupled plasma technique (ICP-AES). The results indicated that the final equilibrium composition of the crystal fiber consisted of SLN and that the length required to reach this final equilibrium composition has affected by the composition of the seed rod. In other words, a seed rod with a higher Li_2O composition required less length to achieve a uniform composition.

The optical properties, such as the UV absorption edge and IR absorption spectrum, were very sensitive to small modifications in the composition of the LN crystal. There have been many studies using different growth techniques where the UV absorption edge in CLN and SLN crystals corresponded to a wavelength where the absorption coefficient was 20 cm^{-1} [3, 10, 11]. The UV absorption edges of CLN and SLN were 320 and 311 nm for the Czochralski method [3] grown from a Li-rich melt; 320 and 306 nm using the flux growth technique [10] grown from CLN melts incorporating different amounts of K_2O from 0 to 10.5 wt%; 322 and 305 nm for the double crucible Czochralski (DCCZ) method [11]; 320 and 305 nm for crystals made produced with VTE [7]; and 318 and 302 nm for Czochralski and TSSG methods [12]. The IR absorption spectrum of the CLN crystal showed a broad IR absorption peak at approximately 3480 cm^{-1}, while the SLN crystal had a sharp peak at 3465 cm^{-1} [3]. The O-H absorption peaks of CLN and SLN were approximately 3480 and 3467 cm^{-1} as measured by Serrano et al. [10], while according to Chen et al. [7] they were the 3481 and 3466 cm^{-1}.

Wöhleche et al. [13] formulated an equation to determine the wavelength of the UV absorption edge of LN crystals with compositions from 48.38 to 50 mol%.

The relationship between the FWHM of the Raman peak at 152 cm^{-1} of the E(TO) mode and the Li_2O composition ranged from sub-congruent to stoichiometric [14, 15, 16]. Complete information about the optical properties of LN crystals within the whole solid solution phase field is not been available. In this study, we utilize the method of Chen et al. [9]. We used the LHPG method to grow LN single crystal fibers with Li_2O compositions ranging from 44 to 50 mol%. We measured the optical properties including the UV absorption edge, IR absorption peak and the FWHM of Raman peak. The relation between the optical properties and the different [Li]/[Nb] ratios is established.

2. Experimental procedure

LN single crystal fibers with different compositions and diameters of around 0.8mm and in 50mm length were grown using the LHPG technique; the pulling direction was along the c-axis. The experimental apparatus used in the present study was developed by Chen and Hu [17, 18] with this apparatus different single crystal fibers, such as $Bi_{12}SiO_{20}$, Mg:$LiNbO_3$, congruent $LiNbO_3$, stoichiometric $LiNbO_3$, Fe:$LiNbO_3$, YVO_4, $BaTiO_3$, Nd:YVO_4, YIG and $Ba_{1-x}Ca_xTiO_3$ fibers can be grown [9, 19-27]. Ceramic plates of LN were prepared. Different proportions of $[Li_2O]/[Nb_2O_5]$ = 42:58, 44:56, 45:55, 46:54, 47:53, 48:52, 48.6:51.4, 49:51, 49.5:50.5, 50:50 and 55:45 were used followed by calcining at 800 ℃ for 24 hours and then sintering. The sintering temperature of a congruent composition was 1070 ℃. For other compositions the temperature was slightly less. The plate was then cut into square source and seed rods about 1 × 1 mm in cross section.

Single crystal fibers were grown from $[Li_2O]/[Nb_2O_5]$ = 44:56, 45:55, 46:54, 47:53, 48:52, 48.6:51.4, 49:51, 49.5:50.5 and 50:50 feed rods at 0.3mm/min. According to equilibrium phase diagram concept [9], the choice at the seed rod reduces the growth time. The phase diagram shows one can grow different compositions at LN single crystals from melts with different Li_2O concentrations. If we want to grow crystals with a Li_2O composition lower than that of the congruent level, the concentration in the molten zone needs be lower than that of the feed rod. Thus to reduce the transition length and the growth time, we must choose a seed rod with a lower composition. To grow crystals higher than the congruent level, the concentration in the molten zone needs to be higher than that at the feed rods; we need to choose seed rods with a higher composition. For convenience, seed rods with $[Li_2O]/[Nb_2O_5]$ compositions = 42:58, 48.6:51.4 and 55:45 were selected. To grow crystal fibers with a composition lower than the congruent level, we used seed rods with a 42 mol% Li_2O composition, while to grow crystal fibers with a composition higher than the congruent level we used seed rods with a composition of 55 mol%. CLN crystal fibers were also grown from congruent seed rod. The heating source was a sealed CO_2 laser operated at a wavelength of 10.6 μm. An X-Ray Single-Crystal Diffractometer (X-Ray/CCD, Siemens Smart CCD) was employed to measure the lattice parameters of the crystal fibers. An infrared imaging system (Inframetrics, Model 760) was used to monitor the molten zone during the growth period. The UV absorption spectrum (Perkin–Elmer Lambda-900) was used to measure the UV absorption edge with light polarized parallel to the optical axis. The UV absorption edge is usually defined as the wavelength corresponding to where the absorption coefficient is equal to 15 or 20 cm^{-1} [3, 12]. In this study, the absorption coefficient used was equal to 20 cm^{-1}. A Fourier-transform infrared spectrometer (Bomem DA8.3) was used to measure the O-H absorption peaks. They ranged from 3400 to 3600 cm^{-1}. A DILOR XY 800 triple grating Raman spectrometer, equipped with a 514.5 nm line Ar^+ ion laser with an output of 200mW was used for the Raman measurements. We calculated the FWHM at 152 cm^{-1} of the E(TO) phonon peak in the X(YZ)X configuration for different Li_2O crystals. The measurements were performed at room temperature.

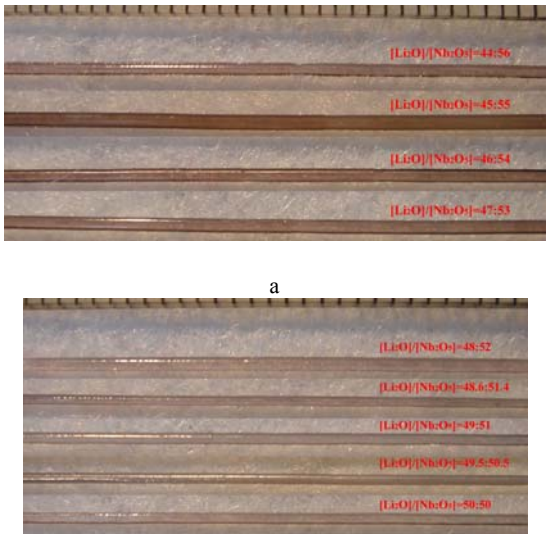

Fig. 1. Photographs of different $LiNbO_3$ fibers grown by the LHPG method: (a) samples with $[Li_2CO_3]/[Nb_2O_5]$ compositions = 44:56, 45:55, 46:54 and 47:53, and (b) $[Li_2CO_3]/[Nb_2O_5]$ = 48:52, 48.6: 51.4 (congruent composition), 49:51, 49.5:50.5 and 50:50 (stoichiometric composition).

3. Results and discussion

Following the method of Chen et al. [9], we used the LHPG method to successfully grow different LN single crystal fibers. Fig. 1 shows the single crystal fibers. Fig. 1 (a) shows the lower Li_2O composition samples (i.e., from 44 to 47 mol%). Note that these crystals although slightly darker are also transparent. This slight darkness disappeared when the Li_2O composition was increased to more than 48mol%; the crystals shown in Fig. 1(b) have

become very transparent.

The X-Ray/CCD results confirmed that the single crystal fibers had a hexagonal LN structure. The lattice parameter results are shown in Fig. 2. In many studies [28-32] X-Ray diffraction has been employed to measure the lattice parameters at different LN single crystals or powders. If we look at Fig. 2, we see that our data are in agreement with other studies. As the structure becomes more perfect it also becomes more rigid. This is why the lattice parameters decrease as the amount of the Li_2O composition of the crystal increases. We also see this tendency in our results, although the lattice parameters did vary insignificantly with the composition. When the Li_2O composition varied from 44 to 50 mol% there was only an approximately 0.01Å distinction of the a-axis and a 0.03 Å distinction of the c-axis. Malovichko et al. [28] developed two approximation equations to describe how the variation of the Li_2O composition will affect the in a-axis and c-axis lattice parameters. These equations suggest that a variation in composition of 1 mol% Li_2O would affect the a-axis by 0.0016Å and the c-axis by 0.006Å, respectively. Thus the lattice parameters for similar compositions are very close. To use these two equations [28] to determine the Li_2O composition are needs to measure the lattice parameters very accurately.

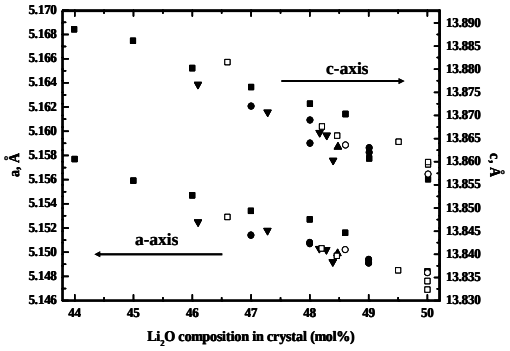

Fig. 2. Lattice parameters for different LN single crystal fibers: (□) Malovichko et al. [28]; (○) Redfirld and Burke [29]; (▼) Grabmaier et al. [30]; (●) Lerner et al. [31]; (▲) Wilkinson et al. [32]; (■) present data.

Fig. 3 shows the wavelength of the UV absorption edge of crystal fibers (an absorption coefficient at 20 cm^{-1}) as a function of Li_2O composition from 44 to 50 mol%. The wavelength of the absorption edge decreased as the amount of the Li_2O composition increased. The variation in the wavelength was very acute when the Li_2O composition was more than 47 mol%, but when the Li_2O composition was less than 47 mol% the wavelength was smoother. A shorter absorption edge wavelength occurred when the SLN was 306 nm, and a longer wavelength, 336.6 nm, occurred when the composition was 44 mol%Li_2O. Previous studies [7, 10, 11] have also shown an SLN absorption edge at 306 and 305 nm; these results are consistent with ours. Wöhlechke et al. [13] used a 2nd order polynomial fit to approximate on Li_2O compositions from 48.83 to 50 mol%. Kovács et al. [12] also used a 2nd order polynomial fit in the range of 47.8 to 50 mol%. The dotted line in Fig. 3 indicates the 2nd order polynomial fit. We found that this fitting line was not suitable for our data. The range of Li_2O compositions in our data was greater than that used in other studies. A composition of less then 47 mol% is not appropriate for a 2nd order polynomial fit. Our data showed that the variation of the UV absorption edge near the minimum and maximum composition would gradually approach a constant value. This characteristic is similar to that of the Gaussian function. Therefore, we select a Gaussian function type to fit our data, which yields the following equation:

$$\lambda_{20}(nm) = 337.66 - 198.65 \times \exp\left[-\frac{(x-59.488)^2}{48.77}\right],$$

where x indicates the Li_2O composition from 44 to 50 mol%. With this equation one can conveniently determine the relation between the wavelength and the Li_2O composition.

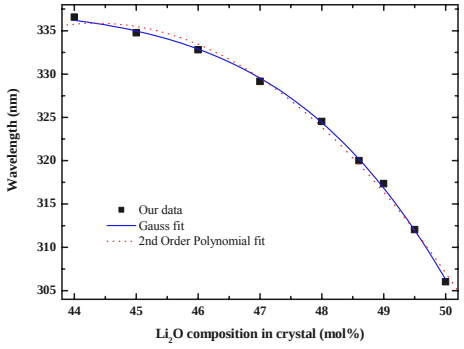

Fig. 3. Wavelength of the UV absorption edge as a function of different compositions of LN single crystal fibers; the absorption coefficient was 20 cm^{-1}.

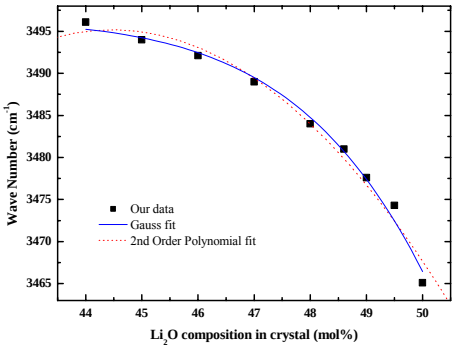

Fig. 4. Wave number of the IR absorption spectrum as a function of different compositions of LN single crystal fibers.

During the growth of the crystal, H atoms enter the crystal by means of vapor, to form an O-H band. In

previous studies [3, 10], the wave number at the strongest IR absorption intensity at this O-H absorption peak is related to [Li]/[Nb] in the LN crystal. In CLN crystal, the O-H absorption peak is at 3481 cm^{-1}, while in the SLN crystal, it is located at 3465 cm^{-1}. We also measured the O-H absorption peaks for the different Li_2O compositions as shown in Fig. 4. We see that our data are in agreement with previous studies of congruent and stoichiometric crystals [3, 10]. As observed from this figure, the wave number of the IR absorption peak is noticeably sensitive to an increase in the Li_2O composition of the crystals. The absorption band shifts to lower frequencies as the Li_2O composition increases. In addition to a polynomial fit for the wave number and Li_2O composition, several other fitting functions were also tested. The results of the second order polynomial and Gaussian fit tests are shown in Fig. 4. The Gaussian fit gave a more accurate approximation for the whole composition range. The Gaussian fit can be described by the following equation:

$$Wave\ \ Number(cm^{-1}) = 3496.44 - 535.61 \times \exp\left[-\frac{(x-63.1457)^2}{59.9678}\right],$$

where x indicates the Li_2O composition from 44 to 50 mol%. With this equation one can conveniently determine the relation between the wave number and the Li_2O composition of LN crystals.

Raman scattering (in the E(TO) mode, at a phonon frequency from 100 to 180 cm^{-1} and in the X(YZ)X configuration), was used to measure the LN single crystal fibers. Measurements were made at room temperature. The results are shown in Fig. 5. The FWHM of the 152 cm^{-1} Raman peak corresponding to Fig. 5 were determined, the results of a comparison between the FWHM and the crystal composition are shown in Fig. 6. The FWHM of the 152 cm^{-1} Raman peak decreased continuously with increasing Li_2O composition. The FWHM variation clearly illustrates that the crystalline structure had become more rigid. Defect structures in the crystal were less when the FWHM was smaller [11]. The intrinsic defect density was greatly reduced when the composition approached stoichiometricity. In other words, crystals become more perfect when the FWHM is smaller. Hence, we can see that the structure of our crystal fibers improved when the Li_2O composition increased. The data referring to each composition in this study were compiled measuring from more than three crystal fibers. Each fiber was measured at more than ten points along the axis. There was 0.5mm between any two points. The range of Li_2O compositions considered in our work was wider then that considered in previous measurements [14, 15, 16]. Our data results are close to previous measurements. Both present and previous results show that the FWHM decreased linearly as the Li_2O composition increased. The dependence, approximated by a linear least square fit yields the following equation:

Li_2O (mol%) = 53.43975 - 0.48496Γ for the 152 cm^{-1} phonon,

where Γ indicates the FWHM for the different LN single crystals. The resolution of FWHM was about 0.1 cm^{-1} for the 152 cm^{-1} phonon. Therefore, the estimated error for the Li_2O composition was about 0.05 mol%. In the above equation, a change in the Li_2O composition of 1 mol% would result in a FWHM variation of over 2 cm^{-1}. Note that the measurement error for each Li_2O composition is small; see Fig. 6. The largest FWHM error was 0.47 cm^{-1} which affected the Li_2O composition by approximately 0.2 mol%. It can be seen that, the composition of the LN crystal can be easily obtained by measuring the 152 cm^{-1} phonon FWHM and comparing it with the detected lattice parameters.

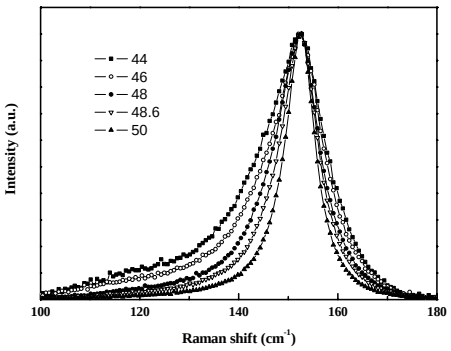

Fig. 5. Raman peak at 152 cm^{-1} of the E(TO) mode in different compositions at LN single crystal fibers.

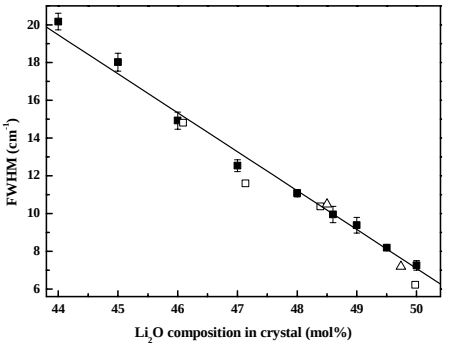

Fig. 6. FWHM of Raman peaks at 152 cm^{-1} in LN for different compositions at crystal fibers: (□) Schlarb et al. [14]; (Δ) Ridah et al. [15]; (■) present data.

4. Conclusions

The present investigation shows that LHPG is a very suitable method for the preparation of incongruent $LiNbO_3$ crystals. Using the LHPG method, we can grow different compositions of $LiNbO_3$ single crystal fibers simply by controlling the composition of the feed rod. The lattice parameters obtained from the X-Ray/CCD measurements can be employed to analyze the Li_2O composition, but

very accurate measurements are required, since the lattice parameters vary only slightly with the composition of LN single crystals. The line of fit between the UV absorption edge or O-H absorption peak and the different compositions at LN crystals tends to follow a Gaussian curve. The relationship between the FWHM of the Raman peak and Li_2O composition was linear. Equations describing the relationship between the optical properties, the UV absorption edge, O-H absorption peak, FWHM of the Raman peak and the composition of the LN crystals can be conveniently used to determine the [Li]/[Nb] ratio in $LiNbO_3$ single crystals.

Acknowledgements

The authors gratefully acknowledge the support of the National Science Council of Taiwan, ROC for their support at this work, through Grant No. NSC 93-2212-E-008-011. We also would like to thank Dr. Hsiang-Lin Liu from the Department of Physics, National Taiwan Normal University, for the loan of the UV absorption spectrum equipment.

References

[1] L. O. Svaasand, M. Eriksrud, G. Nakken, A. P. Grande, J. Crystal Growth **22**, 230 (1974).
[2] J. R. Carruthers, G. E. Peterson, M. Grasso, P. M. Bridenbaugh, J. Appl. Phys. **42**, 1846 (1971).
[3] H. L. Wang, Y. Hang, J. Xu, L. H. Zhang, S. N. Zhu, Y. Y. Zhu, Materials Letters **58**, 3119 (2004).
[4] K. Polgár, Á. Péter, I. Földvári, Opt. Mater. **19**, 7 (2002).
[5] L. Xinan, X. Xu, T.C. Chong, S. Yuan, F. Yu, Y. S. Tay, J. Crystal Growth **260**, 143 (2004).
[6] P. F. Bordui, R. G. Norwood, D. H. Jundt, M. M. Fejer, J. Appl. Phys. **71**, 875 (1992).
[7] Y. Chen, W. Zhang, Y. Shu, C. Lou, Y. Kong, Z. Huang, J. Xu, G. Zhang, Opt. Mater. **23**, 295 (2003).
[8] K. Kitamura, J. K. Yamamoto, N. Iyi, S. Kimura, T. Hayashi, J. Crystal Growth **116**, 327 (1992).
[9] C. Y. Chen, J. C. Chen, Y. J. Lai, J. Crystal Growth, **275**, E769 (2005).
[10] M. D. Serrano, V. Bermúdez, L. Arizmendi, E. Diéguez, J. Crystal Growth, **210**, 670 (2000).
[11] Y. Furukawa, K. Kitamura, S. Takekawa, J. Intell. Mater. Systems Struct., **10**, 470 (1999).
[12] L. Kovács, G. Ruschhaupt, K. Polgár, G. Corradi, M. Wöhlecke, Appl. Phys. Lett. **70**, 2801 (1997).
[13] M. Wöhlecke, G. Corradi, K. Betzler, Appl. Phys. B, **63**, 323 (1996).
[14] U. Schlarb, S. Klauer, M. Wesselmann, K. Betzler, M. Wöhlecke, Appl. Phys. A, **56**, 311 (1993).
[15] A. Ridah, P. Bourson, M. D. Fontana, G. Malovichko, J. Phys. Condens. Matter, **9**, 9687 (1997).
[16] Y. Zhang, L. Guilbert, P. Bourson, K. Polgár, M. D. Fontana, J. Phys.: Condens. Matter, **18**, 957 (2006).
[17] J. C. Chen, C. Hu, J. Crystal Growth **149**, 87 (1995).
[18] J. C. Chen, C. Hu, J. Crystal Growth, **158**, 289 (1996).
[19] J. C. Chen, L. T. Liu, C. C. Young, J. Crystal Growth, **198/199**, 476 (1999).
[20] Y. J. Lai, J. C. Chen, J. Crystal Growth, **198/199**, 531 (1999).
[21] J. C. Chen, Y. C. Lee, J. Crystal Growth, **208**, 508 (2000).
[22] Y. J. Lai, J. C. Chen, J. Crystal Growth, **212**, 211 (2000).
[23] C. H. Huang, J. C. Chen, C. Hu, J. Crystal Growth, **211**, 237 (2000).
[24] J. C. Chen, Y. C. Lee, S. P. Lin, Jpn. J. Appl. Phys. **39**, 1812 (2000).
[25] C. H. Huang, J. C. Chen, J. Crystal Growth, **229**, 184 (2001).
[26] C. C. Hu, J. C. Chen, C. H. Huang, J. Crystal Growth, **225**, 257 (2001).
[27] J. C. Chen, C. Y. Chen, J. Crystal Growth, **236**, 640 (2002).
[28] G. Malovichko, O. Cerclier, J. Estienne, V. Grachev, E. Kokanyan, C. Boulesteix, J. Phys. Chem. Solids, **56**, 1285 (1995).
[29] D. Redfield, W. J. Burke, J. Appl. Phys. **45**, 4566 (1974).
[30] B. C. Grabmaier, W. Wersing, W. Koestler, J. Crystal Growth, **110**, 339 (1991).
[31] P. Lerner, C. Legras, J. P. Dumas, J. Crystal Growth, **3/4**, 231 (1968).
[32] A. P. Wilkinson, A. K. Cheetham, R. H. Jarman, J. Appl. Phys. **74**, 3080 (1993).

*Corresponding author: s0343014@cc.ncu.edu.tw